Neurochem Res (2016) 41:1527–1544
DOI 10.1007/s11064-016-1867-3

ORIGINAL PAPER

A2B5+/GFAP+ Cells of Rat Spinal Cord Share a Similar Lipid Profile with Progenitor Cells: A Comparative Lipidomic Study

Yutaka Itokazu[1,2,3,4] · Nobuyoshi Tajima[2,5] · Laura Kerosuo[2,6] · Pentti Somerharju[2] · Hannu Sariola[2] · Robert K. Yu[3,4] · Reijo Käkelä[1,2]

Received: 8 October 2015 / Revised: 12 January 2016 / Accepted: 8 February 2016 / Published online: 25 February 2016

Abstract The central nervous system (CNS) harbors multiple glial fibrillary acidic protein (GFAP) expressing cell types. In addition to the most abundant cell type of the CNS, the astrocytes, various stem cells and progenitor cells also contain GFAP+ populations. Here, in order to distinguish between two types of GFAP expressing cells with or without the expression of the A2B5 antigens, we performed lipidomic analyses on A2B5+/GFAP+ and A2B5−/GFAP+ cells from rat spinal cord. First, A2B5+/GFAP− progenitors were exposed to the leukemia inhibitory factor (LIF) or bone morphogenetic protein (BMP) to induce their differentiation to A2B5+/GFAP+ cells or A2B5−/GFAP+ astrocytes, respectively. The cells were then analyzed for changes in their phospholipid, sphingolipid or acyl chain profiles by mass spectrometry and gas chromatography. Compared to A2B5+/GFAP− progenitors, A2B5−/GFAP+ astrocytes contained higher amounts of ether phospholipids (especially the species containing arachidonic acid) and sphingomyelin, which may indicate characteristics of cellular differentiation and inability for multipotency. In comparison, principal component analyses revealed that the lipid composition of A2B5+/GFAP+ cells retained many of the characteristics of A2B5+/GFAP− progenitors, but their lipid profile was different from that of A2B5−/GFAP+ astrocytes. Thus, our study demonstrated that two GFAP+ cell populations have distinct lipid profiles with the A2B5+/GFAP+ cells sharing a phospholipid profile with progenitors rather than astrocytes. The progenitor cells may require regulated low levels of lipids known to mediate signaling functions in differentiated cells, and the precursor lipid profiles may serve as one measure of the differentiation capacity of a cell population.

Keywords A2B5 antigen · Astrocyte · Glial fibrillary acidic protein · Glial progenitor/precursor cell · Lipidomics · Mass spectrometry · Phospholipid · Sphingolipid

Abbreviations

BMP	Bone morphogenetic protein
CERS2	Ceramide synthase 2
CNS	Central nervous system
CNTF	Ciliary neurotrophic factor
FA	Fatty acid
gp130	Membrane glycoprotein 130
GFAP	Glial fibrillary acidic protein
GlcCer	Glucosylceramide
GRP	Glial restricted precursor
GRP-LIF	GRP and LIF-stimulated A2B5+/GFAP+ cell
IL-6	Interleukin 6
JAK	Janus kinase

✉ Reijo Käkelä
reijo.kakela@helsinki.fi

[1] Department of Biosciences, University of Helsinki, Biocenter 3, P.O. Box 65, 00014 Helsinki, Finland

[2] Institute of Biomedicine, Department of Biochemistry and Developmental Biology, University of Helsinki, 00014 Helsinki, Finland

[3] Department of Neuroscience and Regenerative Medicine, Medical College of Georgia, Augusta University, Augusta, GA 30912, USA

[4] Charlie Norwood VA Medical Center, Augusta, GA 30904, USA

[5] Present Address: Department of Physiology, Kanazawa Medical University, Ishikawa 920-0293, Japan

[6] Present Address: Division of Biology and Biological Engineering, California Institute of Technology, Pasadena, CA 91125, USA

LIF	Leukemia inhibitory factor
MUFA	Monounsaturated fatty acid
PC	Phosphatidylcholine
PCA	Principal component analysis
PE	Phosphatidylethanolamine
PGE2	Prostaglandin E2
PI	Phosphatidylinositol
PL	Phospholipid
PS	Phosphatidylserine
PUFA	Polyunsaturated fatty acid
SFA	Saturated fatty acid
SIMCA	Soft independent modeling of class analogy
SL	Sphingolipid
SM	Sphingomyelin
STAT	Signal transducer and activator of transcription

Introduction

The nervous tissue is composed of neurons, which transmit impulses, and glial cells (i.e., astrocytes, oligodendrocytes, and microglia derived from circulation), which provide trophic support and protection for neurons. Recently, astrocytes were found to be responsible for a wide variety of essential functions in the central nervous system (CNS), including regulation of neurogenesis, synaptogenesis, and development of the neural circuit [1–4]. On the other hand, during early stages of neurodegenerative disorders of the CNS, activated astrocytes may participate in limiting tissue injury, reducing inflammation, and taking part in reestablishing the blood–brain barrier. At later stages, however, astrocytes may delay CNS recovery since they have been suggested to contribute to inhibition of axonal regeneration [1–4].

A2B5 antigens, including the c-series gangliosides such as GT3, GT1c and GQ1c, are well known markers for immature progenitor cells in the nervous system [5–8]. These c-series gangliosides are phylogenetically conserved and developmentally regulated, and are most abundant in the brain of lower vertebrates, such as fish, and the brain of mammalian embryos. In adult zebrafish brain, c-series gangliosides comprise up to 70 % of the total gangliosides [9]. Accordingly, damaged zebrafish brain have high regeneration capacity and the brain is rich in A2B5+ cells [10]. In proliferating neural stem cells of mammals, ST-III, an enzyme for the synthesis for c-series gangliosides (A2B5 antigens), is highly expressed [11]. In maturing mammalian brain, the concentration of c-series gangliosides decreases drastically [12–15], and this decrease in the synthesis of c-series gangliosides is compensated by a pathway shift in favor of the accretion of a- and b-series gangliosides [15–17]. Glial restricted precursors (GRPs) are experimentally characterized based on their expression of A2B5 antigens [18], but it is still uncertain whether GRPs indeed exist in vivo. Thus additional chemical analyses to characterize these cells beyond those known cell surface marker molecules are needed. The present study focuses on phospholipids (PLs), sphingolipids (SLs) and fatty acids (FAs) that play a significant role in participating in signaling of neural cells [19].

The interleukin (IL)-6 family of cytokines, such as the leukemia-inhibitory factor (LIF) and the ciliary neurotropic factor (CNTF), have been functionally implicated in astrocytic differentiation [20]. Both cytokines share common signaling platforms, i.e., the membrane glycoprotein 130 (gp130) and the LIF receptor (LIFR) [21]. Astrocytic differentiation is also regulated by another group of cytokines, i.e., the bone morphogenetic proteins (BMPs) that are members of the transforming growth factor β (TGFβ) pathway, and can thereby induce differentiation and development of astrocytes [22, 23]. The BMP pathway is mediated by heterotetrameric serine/threonine kinase receptors and their downstream transcription factors Smads.

Our knowledge on the role of lipids in modulating cytokine-induced responses in stem cell differentiation is still fragmentary. Since most growth factor receptors are localized on the plasma membrane, it is reasonable to assume that they interact with membrane lipids in a specific manner. The SL and cholesterol-enriched plasma membrane microdomains (lipid rafts) with specific protein and lipid composition are thought to be important for the regulation of many biological and pathological processes [24–26]. First, membrane microdomains may be required for these signaling pathways since destabilizing lipid rafts by removal of membrane cholesterol was reported to attenuate LIF-induced phosphorylation of STAT3 and Akt in murine embryonic stem cells [27]. In addition, lipid rafts were found to contribute to activation of Ras-MAPK pathway and proper adhesion properties of murine neuroepithelial cells [28]. Second, prostaglandin E2 (PGE2) secretion is IL-6-dependent and regulates differentiation of embryonic stem cells through BMP/Smad signaling [29, 30]. Since the precursor for PGE2 production, arachidonic acid (20:4n-6), is released from membrane PLs, the availability of this specific polyunsaturated fatty acid (PUFA) for cellular phospholipases likely modulates this signaling. In addition, many more lipid-mediated effects are possible, and may originate either from membrane structural changes or alterations in producing specific signaling lipids. Therefore cellular lipid composition, as revealed in this study, can be considered as an important mediator of these lipid signaling.

LIF signaling has been reported to produce GFAP+ progenitor cells, while BMP signaling promotes GFAP+

mature astrocytes [31]. Even though astrocytes represent the largest cell population in CNS [32], the lipidomes of GRPs and GFAP+ cells derived thereof are not known. Recently lipidomic profiling of PLs has been successfully used for defining subpopulations in breast cancer cells [33]. Showing great promise as tools for regenerative medicine, transplanted astrocytes derived from GRPs were found to promote recovery from neurodegenerative disorders in animal models [34–45]. However, the lipid profiles of isolated GRPs and possible lipidomic changes upon their differentiation have not been studied in detail. Novel lipid markers for distinct astrocyte subpopulations should provide a useful tool for selecting cells with proper functionality for neurodegenerative therapy purposes. We analyzed the lipid profiles of GRPs (A2B5+/GFAP−) isolated from the spinal cord of E13.5 rat embryos. Differentiation of GRPs to GFAP+ cells was induced using either LIF or BMP, and the subsequent alterations in the profiles of PLs, simple SLs and FAs were determined. Interestingly, we found that PL species profiles of BMP-induced A2B5−/GFAP+ astrocytes were distinct from GRPs and LIF-stimulated A2B5+/GFAP+ cells. Our lipidomic analyses suggest that A2B5+/GFAP+ cells (i.e., type 2 astrocytes) express a lipid profile more similar to that of immature cells than that of A2B5−/GFAP+ astrocytes (i.e., type 1 astrocytes). Furthermore, it may be common for progenitor cells to maintain specific lipid composition that does not provide high levels of precursors for lipid mediators that would drive cell differentiation.

Experimental Procedure

Glial Progenitors and Differentiation

GRPs were isolated from E13.5 rat spinal cord as cells being positive for the glial progenitor marker, A2B5, and negative for the neuronal progenitor marker, polysialic acid-neural cell adhesion molecule (PSA-NCAM) [46]. Neuron-restricted precursors were removed by negative selection using anti-PSA-NCAM microbeads (Milteny Biotec, Bergisch-Gladbach, Germany) on a magnetic sorting device (MACS, Milteny Biotec), and then the A2B5+ cells were obtained using anti-A2B5 microbeads (Milteny Biotec). The isolated GRPs were plated on dishes or coverslips that had been coated with poly-D-lysine (Sigma-Aldrich, St. Louis, MO) and laminin (BD Biosciences, San Jose, CA) and cultured in DMEM/F12 medium (Invitrogen, Carlsbad, CA) supplemented with B27 (Invitrogen), N2 (Invitrogen), 1 mg/ml of BSA (Sigma-Aldrich), and 20 ng/ml of basic fibroblast growth factor-2 (FGF-2) (Peprotech, Rocky Hill, NJ). GRPs have successfully been induced into GFAP+ cells [35, 39, 46–48]. In this study, GRPs were treated with LIF (Sigma-Aldrich) for 5 days to obtain A2B5+/GFAP+ cells or with BMP-2 (Peprotech) for 5 days to obtain A2B5-/GFAP+ astrocytes. The use of experimental animals was approved by the Institutional Animal Care and Use Committee at the University of Helsinki.

Immunocytochemistry

Cells were fixed in 4 % paraformaldehyde for 20 min at room temperature, washed three times with PBS, permeabilized for 3 min in PBS containing 0.1 % Triton, and blocked with 5 % goat serum and 1 % BSA for 30 min. The treated cells were then incubated with antibodies overnight in a chamber with a humid atmosphere at 4 °C. The primary antibodies used were an anti-A2B5 mouse antibody (Milteny Biotec) and an anti-GFAP rabbit antibody (Dako, Glostrup, Denmark). After incubation with the primary antibodies, the cells were washed three times with PBS and incubated with Alexa 488 anti-mouse or Alexa 543 anti-rabbit antibodies (Invitrogen) for 2 h in the dark, washed and then incubated with 4,6-diamidino-2-phenylindole (DAPI, Invitrogen) for 5 min to stain the nuclei. Confocal images were acquired with an LSM 510 Meta microscope (Carl Zeiss GmbH, Jena, Germany).

Lipid Analysis by Mass Spectrometry and Gas Chromatography

The total cellular lipids were extracted as described [49], spiked with internal standards, evaporated to near dryness, and dissolved in chloroform/methanol 1:2 for direct infusion experiments. Several internal standards were used to correct for the effects of the polar head group and acyl chain length on the instrument response [50–54]. Just prior to analysis, 1 % NH_4OH was added and the lipid extract was infused to the electrospray source of a Quattro Micro triple quadrupole mass spectrometer (Micromass, Manchester, UK) at the flow rate of 8 µl/min. The collision energy of the instrument was set to 25–65 eV either in the negative or positive ion mode. Argon was used as the collision gas and different lipid species were selectively detected based on specific precursor ions or neutral loss MS/MS scanning modes [55, 56]. The acyl chain compositions of the major lipid species were determined by product ion analysis. The mass spectra were processed using the MassLynx software (Micromass, Manchester, UK) and the individual lipid species were quantified using appropriate internal standards with the LIMSA software [57]. The species abbreviation was as follows: [total carbon number in the chains]:[total number of double bonds in the chains]. The concentrations of the lipid classes were obtained by summing the concentrations of the individual molecular species in the class.

The lipid FA residues were determined as methyl ester derivatives by gas chromatography [58], the FA composition was calculated as molar percentage, and the FAs were abbreviated as: [carbon number]:[number of double bonds] n-[position of the first double bond calculated from the methyl end] (e.g., 20:4n-6).

Statistical Analysis

Data are expressed as the mean ± SE of the mean (SEM) calculated from three independent experiments. The statistical significance of compositional differences was determined using one-way ANOVA followed by Tukey's post hoc multiple comparison test, unpaired two-tailed Student's *t* test, or by multivariate principal component analysis (PCA) [59]. Prior to PCA, the molar percentages were logarithmically transformed to prevent the abundant components (with a larger variance) from dominating the analysis. In PCA the samples originally positioned in multidimensional space (as many coordinates as chemical components analyzed) were plotted in a newly formed two-coordinate system of principal components, PC1 and PC2. The PC1 accounted for as much of the original data variability as possible and the PC2 explained as much as possible of the remaining variation uncorrelated with the variation already explained by PC1. To quantify the compositional differences between the samples from different experimental groups (described by a PCA biplot), space-filling models were created for two of the groups at a time and the distances of the samples to these two models were computed using soft independent modeling of class analogies (SIMCA). Statistically significant difference at a given P-value necessitates that none of the samples is classified as belonging to both of the group models. In all statistics employed, a P value <0.05 was regarded as significant. The multivariate computations were performed using the SIRIUS 8.5 program package (Pattern Recognition Systems, Bergen, Norway).

Results

Astrocyte Differentiation from Glial Restricted Precursors

GRPs can be recognized in vitro based on the expression of A2B5 in neural epithelial cells [18]. LIF signaling has been reported to produce GFAP+ progenitor cells, while BMP signaling promotes GFAP+ mature astrocytes [31]. First, we isolated A2B5 positive and PSA-NCAM negative GRPs from the spinal cord of rat embryos (Fig. 1a, A2B5+/GFAP− progenitors). Then we treated GRPs with LIF for 5 days. Immunocytochemical analysis demonstrated that all LIF-stimulated cells were A2B5+/GFAP+ expressing cells (Fig. 1b). Alternatively, we exposed these cells with BMP for 5 days. Immunocytochemical experiments confirmed that the expression of A2B5 disappeared in all BMP-induced A2B5−/GFAP+ astrocytes (Fig. 1c). The GRPs (A2B5+/GFAP− progenitors), LIF-stimulated A2B5+/GFAP+ cells, and BMP-induced A2B5−/GFAP+ astrocytes were analyzed for lipid profiles as described below.

Lipid Class Composition

At the level of lipid classes, the total proportion of diacyl phosphatidylcholine (hereafter PC) decreased and ether phospholipids (alkyl-acyl phosphatidylcholine, PCa and alkenyl-acyl phosphatidylethanolamine, PEp), and sphingomyelin (SM) showed a tendency to increase from GRPs to the differentiated cells (Fig. 2a, c). Multivariate statistical analysis PCA showed that the LIF-stimulated A2B5+/GFAP+ cells had a lipid class composition more similar to that of GRPs rather than BMP-induced A2B5−/GFAP+ astrocytes (Fig. 2c). The compositional differences were quantified by SIMCA, which confirmed that the BMP-induced A2B5−/GFAP+ astrocytes had a lipid composition significantly different from that of the GRPs and LIF-stimulated A2B5+/GFAP+ cells. However, the latter two had a similar lipid composition (Fig. 2d). Thus, for further univariate statistical analysis (Student's *t* test, with the $P < 0.05$ criterion) the lipid class data of GRPs and LIF-stimulated A2B5+/GFAP+ cells (GRP-LIF) were combined and compared with those for BMP-induced A2B5−/GFAP+ astrocytes (GRP-LIF vs. BMP). The relative amount of PC+PCa was significantly reduced from GRP-LIF (51.53 ± 0.68 mol %) to BMP-induced A2B5−/GFAP+ astrocytes (46.63 ± 1.90 mol%). Particularly, the relative amount of PC was significantly reduced from GRP-LIF (45.42 ± 1.04 mol%) to BMP-induced A2B5−/GFAP+ astrocytes (38.87 ± 2.98 mol%). In parallel, the total proportions of PCa and PEp classes were slightly elevated, and phosphatidylserine (PS) increased by 2-fold from GRP-LIF (2.61 ± 0.41 mol%) to BMP-induced A2B5−/GFAP+ astrocytes (4.07 ± 0.30 mol%; $P = 0.054$). In addition, the SM/(PC+PCa) ratio was significantly elevated from GRP-LIF (0.13 ± 0.01) to BMP-induced A2B5−/GFAP+ astrocytes (0.20 ± 0.03). SM, ceramide (Cer) and glucosylceramide (GlcCer) were combined as SL. The level of SL was significantly elevated from GRP-LIF to BMP-induced A2B5−/GFAP+ astrocytes, also seen as elevated SL/(PC+PCa) ratio (0.14 ± 0.01 vs. 0.21 ± 0.03, respectively). In addition, the lysophosphatidylcholine (LysoPC) content of the LIF-stimulated A2B5+/GFAP+ cells was significantly higher than the totals of the other cells (one-way ANOVA

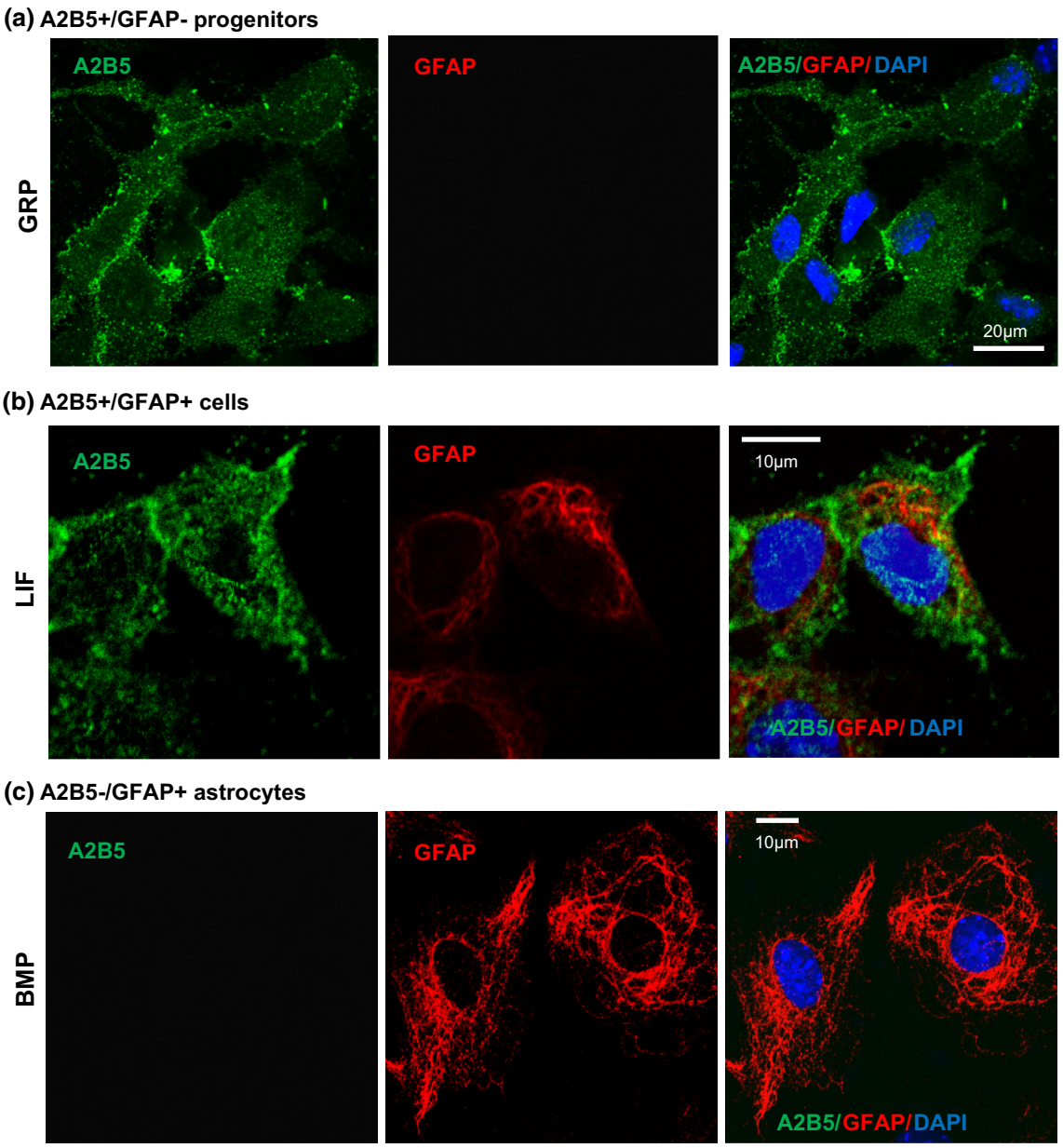

Fig. 1 The expressions of glial lineage markers A2B5 and GFAP. *Green* staining represents A2B5, *red* is GFAP and *blue* is the nuclear stain DAPI. **a** Glial restricted precursors (GRPs) express A2B5 but not GFAP (A2B5+/GFAP−). **b** LIF-stimulated A2B5+/GFAP+ cells express both A2B5 and GFAP. **c** BMP-induced A2B5−/GFAP+ astrocytes strongly expressed GFAP but not A2B5. *Scale bar a* 20 μm, *b* 10 μm, *c* 10 μm (Color figure online)

followed by Newman-Keuls test of means, $P < 0.05$) (Fig. 2b).

PC and PCa Molecular Species Profiles

Typical MS spectra for the choline lipids (i.e., PC, PCa, LysoPC and SM) are presented in Fig. 3 (panels a, b). The quantitative changes of PC and PCa species and multivariate comparison of the PC+PCa composition are shown in Fig. 3c–e, and identification of the acyl chains and univariate statistics are shown in Table 1. BMP-induced A2B5−/GFAP+ astrocytes contained elevated levels of PC 32:0, 36:4 and 38:4, while the levels of monounsaturated 32:1 and 36:1 were decreased (Fig. 3c, e). The 20:4n-6 containing PC species (36:4+38:4) were significantly elevated from GRP-LIF (9.56 ± 0.96 mol%) to BMP-induced A2B5-/GFAP+ astrocytes (13.40 ± 0.44 mol%) (*t* test, Fig. 3c). Among the PCa species, 34:2a and 36:2a were significantly decreased and 36:4a was significantly elevated from GRP-LIF to BMP-induced A2B5−/GFAP+

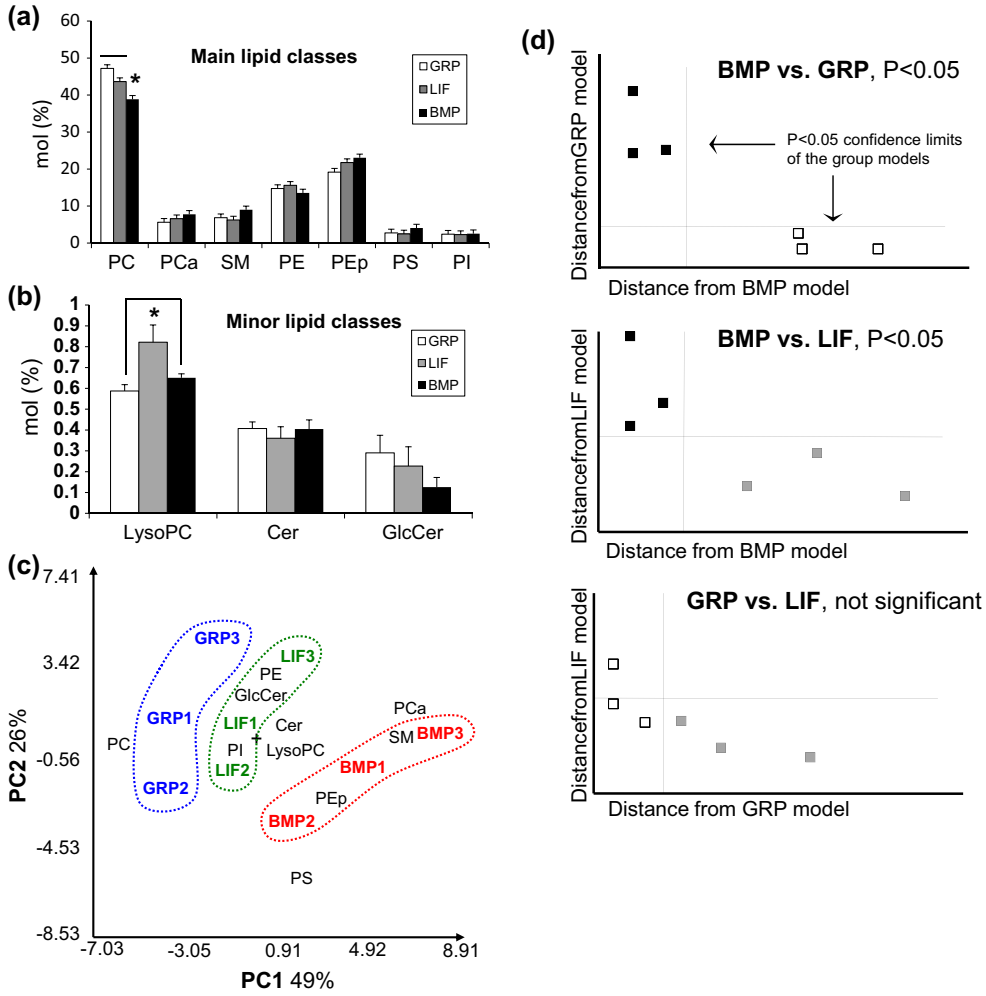

Fig. 2 Lipid compositions of GRP, LIF-stimulated A2B5+/GFAP+ cells and BMP-induced A2B5-/GFAP+ astrocytes. The molar percentages of individual molecular species in a given lipid class were summed up for major (**a**) and minor (**b**) classes. Statistically significant (*t* test, $P < 0.05$) difference was marked with *asterisk*, and the comparison groups were indicated by *horizontal lines* (covering one or a combined group). **c** Principal component analysis (PCA) biplot (of scores and loadings) of the lipid class data. The *colored* characters indicate individual cell cultures (e.g., GRP1). Three individual experiments were performed (the number following the cell line abbreviation represents an individual experiment). **d** SIMCA analyses, which followed PCA, showed that the lipid class composition in BMP was statistically different from those in GRP and LIF ($P < 0.05$). However, the composition in GRP and LIF did not differ at this risk level. *PC* diacylphosphatidylcholine, *PCa* alkyl-acyl phosphatidylcholine, *SM* sphingomyelin, *PE* diacyl phosphatidylethanolamine, *PEp* alkenyl-acyl phosphatidylethanolamine (plasmalogen), *PS* phosphatidylserine, *PI* phosphatidylinositol, *LysoPC* lysophosphatidylcholine, *Cer* ceramide, *GlcCer* glucosylceramide, *GRP* glial restricted precursor, *LIF* LIF-stimulated A2B5+/GFAP+ cells, *BMP* BMP-induced A2B5−/GFAP+ astrocytes

astrocytes (Fig. 3d, Table 1). The PCA confirmed that in the BMP-induced A2B5−/GFAP+ astrocytes highly unsaturated PC and PCa species dominated at the expense of the di-unsaturated species (i.e., mainly species with two monounsaturated acyl chains) (Fig. 3e). The PC+PCa compositions in the LIF- and BMP-induced A2B5−/GFAP+ astrocytes were significantly different (SIMCA). When the PC and PCa species were grouped based on their degree of unsaturation, the diunsaturated species were significantly decreased from GRP-LIF (19.82 ± 0.68 mol%) to BMP-induced A2B5−/GFAP+ astrocytes (15.99 ± 1.19 mol%) (Fig. 3f), while the polyunsaturated species were increased from GRP-LIF (28.75 ± 1.88 mol%) to BMP-induced A2B5−/GFAP+ astrocytes (33.93 ± 0.9 mol%; $P = 0.108$).

PE Species

The PEp class was increased from GRP to LIF-stimulated A2B5+/GFAP+ cells and BMP-induced A2B5−/GFAP+ astrocytes (Fig. 2a). A typical MS spectrum for phosphatidylethanolamine diacyl species (hereafter PE) is

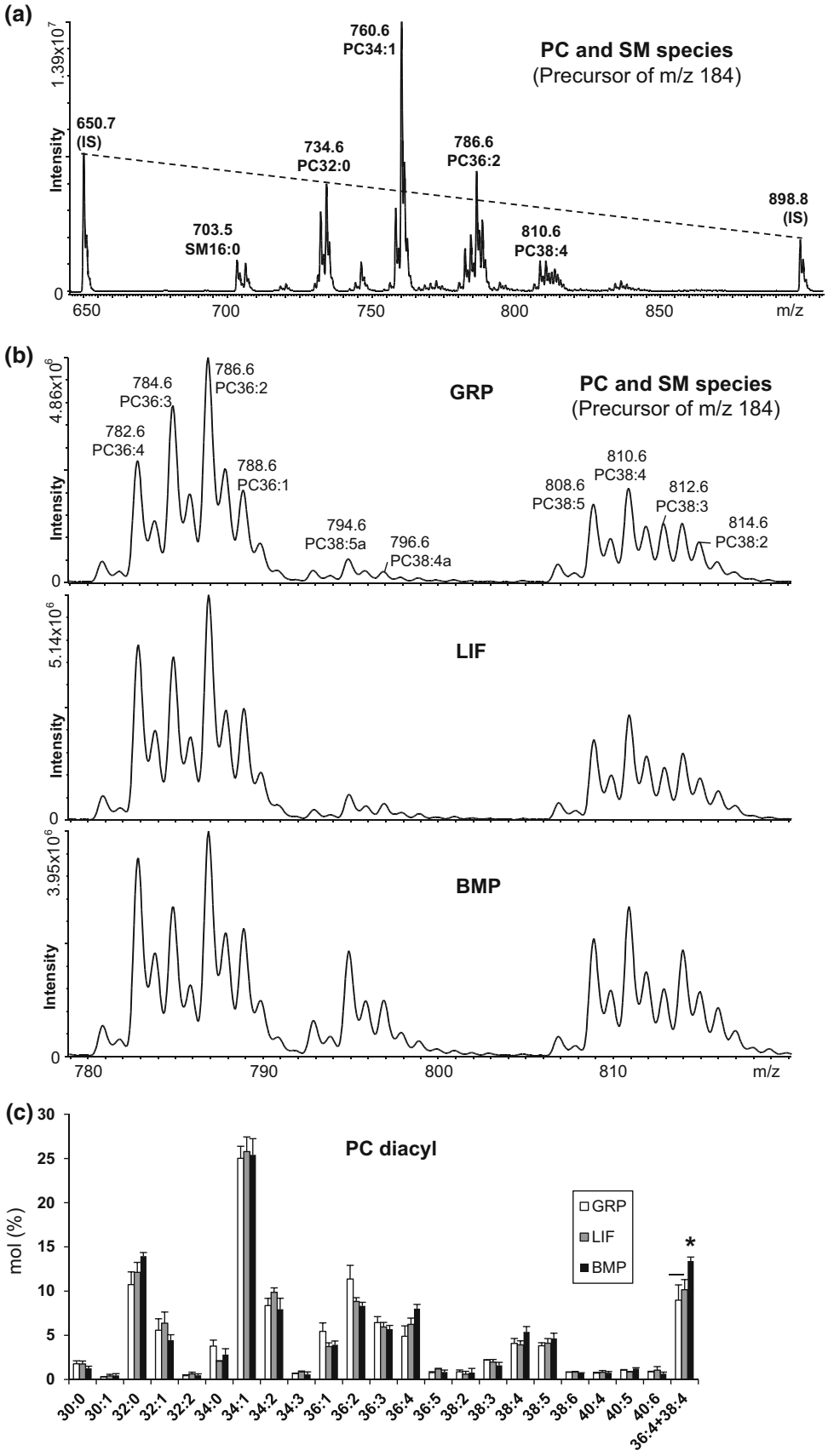

Fig. 3 Mass spectra for PC and SM molecular species. **a** Full-range spectrum showing also the PC internal standards (IS) and a *dashed calibration line* in GRPs. **b** Mass spectra showing selected PC species in GRPs (GRP), LIF-stimulated A2B5+/GFAP+ cells (LIF) or BMP-induced A2B5-/GFAP+ astrocytes (BMP). Percental abundances of the principal PC (**c**) and PCa (**d**) species in GRP, LIF-stimulated A2B5+/GFAP+ cells or BMP-induced A2B5−/GFAP+ astrocytes. **e** PCA biplot of the combined PC+ PCa species data using the 25 quantitatively largest species as loadings, and significant group differences indicated by SIMCA as insert. **f** Molar proportions of saturated (SAT), monounsaturated (MONO), diunsaturated (DI, mainly species that contain two monounsaturated acyl chains) and polyunsaturated (POLY) species of PC. Three individual experiments were performed. In *bar graphs* (**c**, **d**, **f**), statistically significant (*t* test, $P < 0.05$) difference was marked with *asterisk*, and the comparison groups were indicated by *horizontal lines* (covering one or a combined group)

Fig. 3 continued

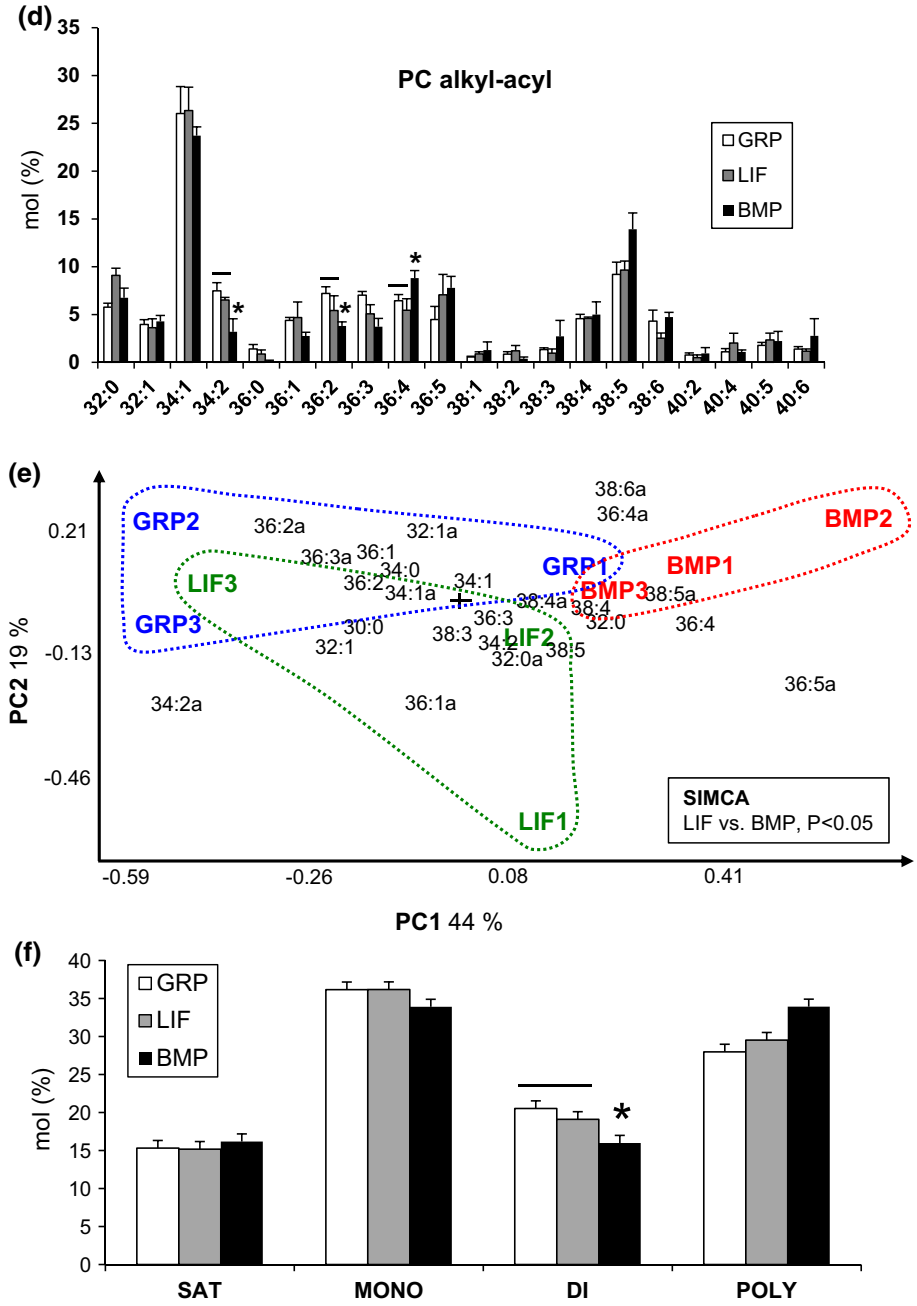

presented in Fig. 4a, quantitative changes of PE and PEp species and multivariate comparison of the PE+PEp composition in Fig. 4b–d, and the identified acyl chains and univariate statistics in Table 2. PE species (36:1 and 40:4) were significantly elevated from GRP-LIF to BMP-induced A2B5−/GFAP+ astrocytes, while the 34:2, 36:3 and 38:6 were significantly decreased in parallel (Fig. 4b; Table 2). Among PEp molecular species, the 36:3p species was significantly decreased and 36:4p significantly increased from GRP-LIF to BMP-induced A2B5−/GFAP+ astrocytes (Fig. 4c; Table 2). The PCA confirmed the trend of BMP-induced A2B5−/GFAP+ astrocytes having more polyunsaturated species with 4–5 double bonds (total) and less with 2–3 double bonds in their acyl chains (Fig. 4d). The PE+PEp species composition of BMP-induced A2B5-/GFAP+ astrocytes significantly differed from those of the GRPs and LIF-stimulated A2B5+/GFAP+ cells, and the latter two had very similar compositions (SIMCA). When compared to LIF-stimulated A2B5+/GFAP+ cells, the BMP-induced

Table 1 Principal phosphatidylcholine (PC and PCa) molecular species

Molecular species	Identified acyl chain			*m/z* (+)	Molecular species	Identified acyl chain		*m/z* (+)	$P < 0.05$
PC diacyl species (PC)	*Acyl/acyl*				*PC alkyl-acyl species (PCa)*	*Ether/acyl*			
30:0	14:0/16:0			706.5	32:0	16:0a/16:0		720.6	
30:1	14:0/16:1			704.5	32:1	16:0a/16:1		718.6	
32:0	16:0/16:0			734.6	34:1	16:0a/18:1	18:1a/16:0	746.6	
32:1	16:0/16:1			732.6	34:2	16:0a/18:2	18:1a/16:1	744.6	GRP-LIF vs BMP
32:2	16:1/16:1			730.5	36:0	18:0a/18:0		776.7	
34:0	16:0/18:0			762.6	36:1	18:0a/18:1	18:1a/18:0	774.6	
34:1	16:0/18:1			760.6	36:2	16:0a/20:2	18:1a/18:1	772.6	GRP-LIF vs BMP
34:2	16:0/18:2	16:1/18:1		758.6	36:3	18:1a/18:2	16:0a/20:3	770.6	
34:3	16:1/18:2			756.6	36:4	16:0a/20:4		768.6	GRP-LIF vs BMP
36:1	18:0/18:1	16:0/20:1		788.6	36:5	16:0a/20:5		766.6	
36:2	18:1/18:1	16:0/20:2	18:0/18:2	786.6	38:1	18:0a/20:1		802.7	
36:3	18:1/18:2	16:0/20:3		784.6	38:2	18:0a/20:2	16:0a/22:2	800.7	
36:4	18:2/18:2	16:0/20:4		782.6	38:3	18:0a/20:3	18:1a/20:2	798.6	
36:5	16:1/20:4	16:0/20:5		780.6	38:4	18:0a/20:4	18:1a/20:3	796.6	
38:2	18:0/20:2	16:0/22:2		814.6	38:5	18:1a/20:4	16:0a/22:5	794.6	
38:3	18:1/20:2	18:0/20:3		812.6	38:6	18:1a/20:5	16:0a/22:6	792.6	
38:4	18:0/20:4	18:2/20:2		810.6	40:2	18:0a/22:2		828.7	
38:5	18:1/20:4	16:0/22:5		808.6	40:4	18:0a/22:4		824.7	
38:6	18:2/20:4	16:1/22:5		806.6	40:5	18:1a/22:4	18:0a/22:5	822.6	
40:4	18:0/22:4	20:2/20:2		838.6	40:6	18:1a/22:5	18:0a/22:6	820.6	
40:5	18:0/22:5	18:1/22:4	20:1/20:4	836.6					
40:6	18:1/22:5	18:2/22:4	18:0/22:6	834.6					

Statistical significance (*P*) was determined using one-way ANOVA followed by Tukey's post hoc multiple comparison test or comparing combined group of GRPs and LIF-stimulated A2B5+/GFAP+ cells with BMP-induced A2B5−/GFAP+ astrocytes by unpaired two-tailed Student's *t* test. Data are from 3 independent experiments (n = 3). sn-1 Ether linkage (alkyl chain) is indicated with the letter a (e.g. 18:1a/16:0)

A2B5−/GFAP+ astrocytes exhibited a significant decrease (from 17.19 ± 0.42 to 14.25 ± 0.9 mol%) of PE+PEp diunsaturated species and a significant increase of the polyunsaturated species (from 68.01 ± 0.41 to 72.31 ± 1.16 mol%; Fig. 4e).

PS and PI Species

The most abundant PS species of the studied cells was 36:1 (43–47 mol%) followed by two polyunsaturated species 38:3 and 38:4, both exceeding 10 mol% (Fig. 5a). The

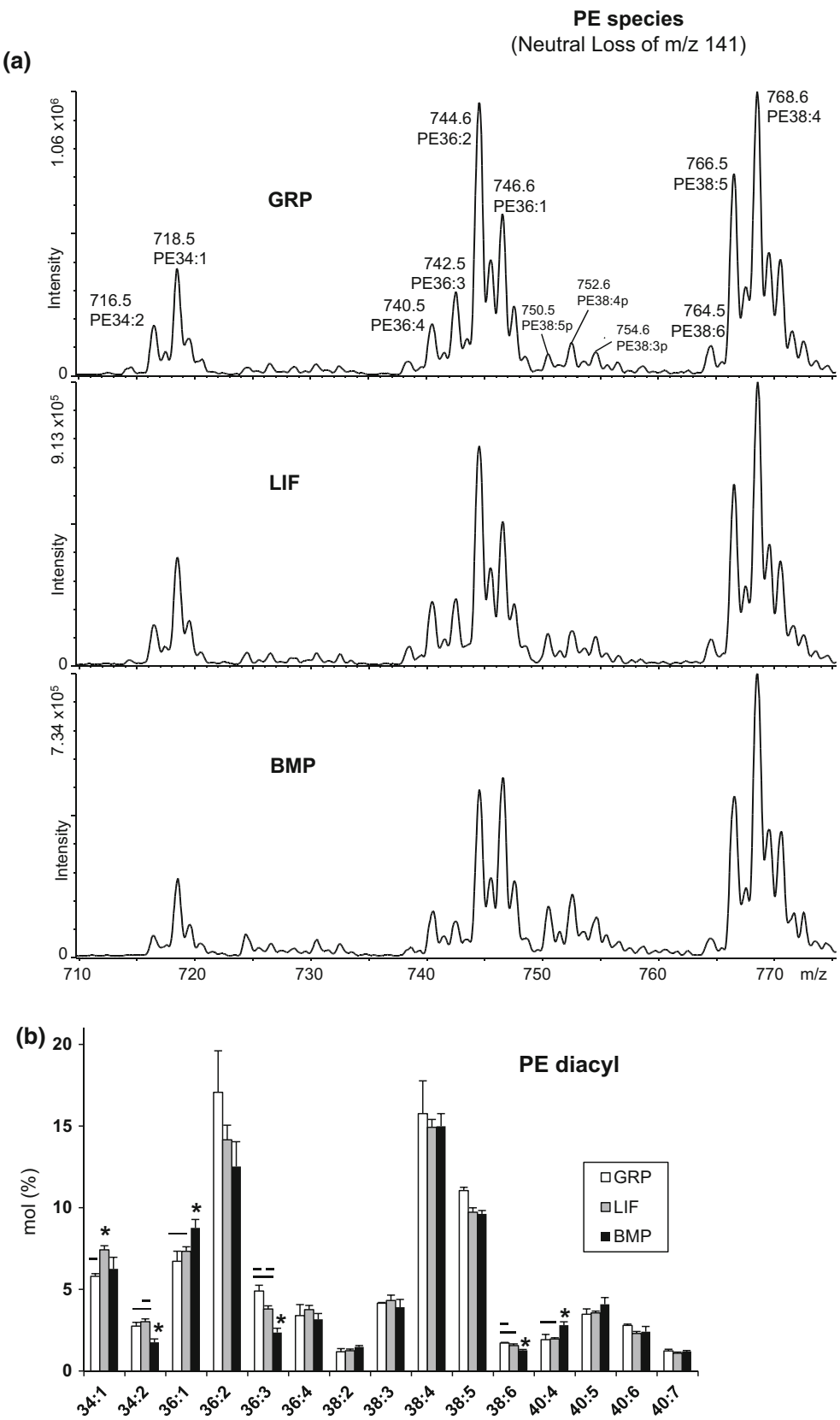

Fig. 4 Mass spectrum showing the principal PE molecular species in GRP, LIF-stimulated A2B5+/GFAP+ cells or BMP-induced A2B5-/GFAP+ astrocytes (**a**). Percental abundances of the principal PE (**b**) and PEp (**c**) species in GRP, LIF-stimulated A2B5+/GFAP+ cells or BMP-induced A2B5−/GFAP+ astrocytes. **d** PCA biplot of the combined PE+PEp species data, and significant group differences indicated by SIMCA as *insert*. **e** Molar proportions of saturated (SAT), monounsaturated (MONO), diunsaturated (DI, mainly species that contain two monounsaturated acyl chains) and polyunsaturated (POLY) species of PE. Three individual experiments were performed. In *bar graphs* (**b**, **c**, **e**), statistically significant (*t* test, $P < 0.05$) difference was marked with *asterisk*, and the comparison groups were indicated by *horizontal lines* (covering one or a combined group)

Fig. 4 continued

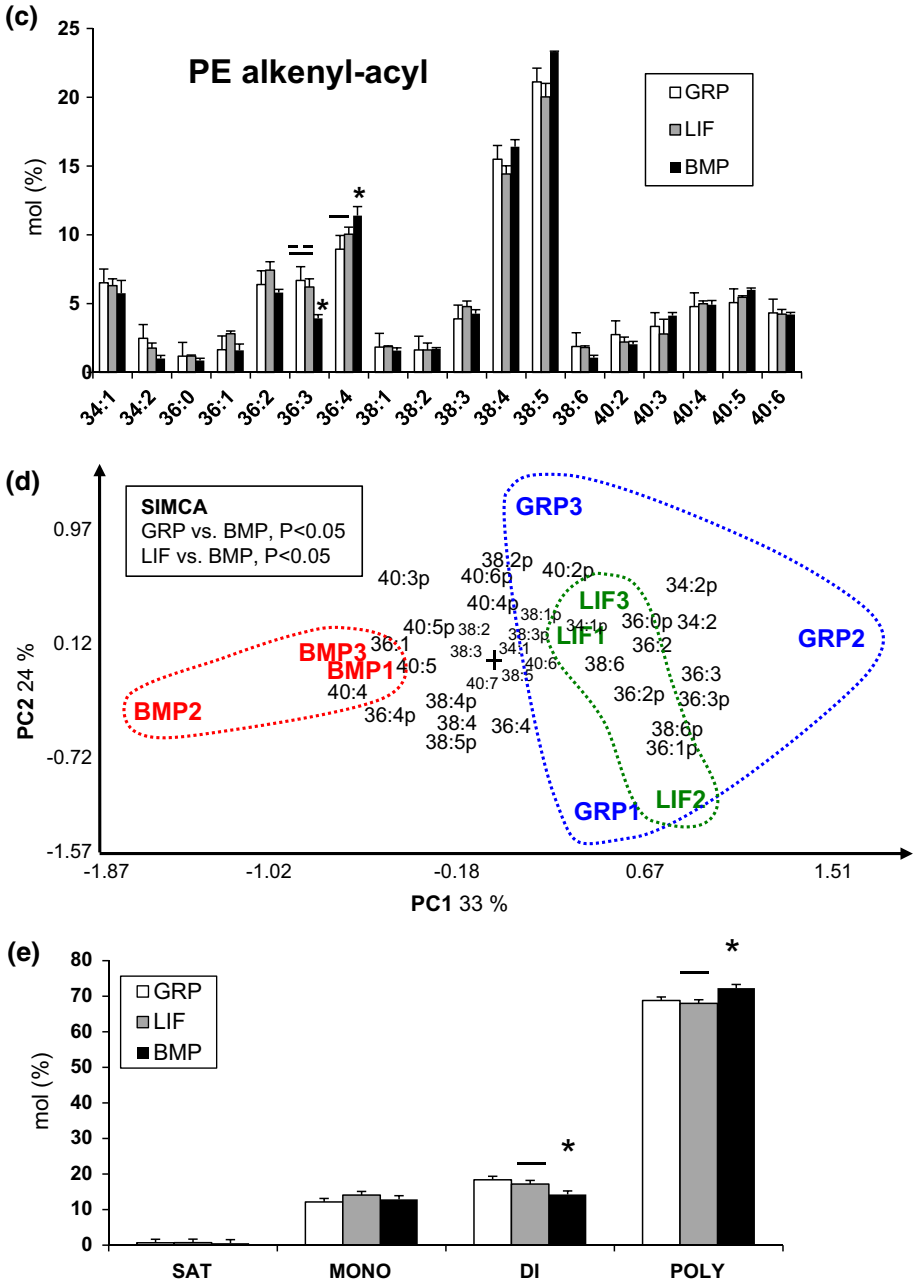

major phosphatidylinositol (PI) species was 38:4 (53–56 mol%, Fig. 5b). The species compositions of PS and PI showed only slight changes from GRPs to LIF-stimulated A2B5+/GFAP+ cells or BMP-induced A2B5-/GFAP+ astrocytes (Fig. 5a, b; Table 3).

LysoPC, SM, Ceramide, Glucosylceramide Molecular Species and Fatty Acyl Residues

The main LysoPC species in the studied cells were 16:0 (33–38 mol%) and 18:1 (25–30 mol%). In SM, the species, 16:0 (25–28 mol%), 24:1 (23–25 mol%) 18:0 (11–16 mol%), and 22:0 (9–16 mol%) were the most abundant. In Cer of LIF-stimulated A2B5+/GFAP+ cells, the content of the 24:0 species was significantly higher and that of 16:0 lower compared to the combined values of GPRs and BMP-induced A2B5−/GFAP+ astrocytes (Fig. 5e, detailed data of all the minor lipids are shown in Fig. 5; Table 4). Molar proportions of the most abundant acyl residues (including alkenyl chains) of the total lipids are shown in Table 5.

Table 2 Principal phosphatidylethanolamine (PE and PEp) molecular species

Molecular species	Identified acyl chain			*m/z*	$P < 0.05$
PE diacyl species (PE)	*Acyl/acyl*			*m/z (+)*	
34:1	16:0/18:1			718.5	GRP vs LIF,
34:2	16:0/18:2	16:1/18:1		716.5	LIF vs BMP, GRP-LIF vs BMP
36:1	18:0/18:1	16:0/20:1		746.6	GRP-LIF vs BMP
36:2	18:1/18:1	16:0/20:2	18:0/18:2	744.6	
36:3	18:1/18:2	16:0/20:3		742.5	GRP vs BMP, LIF vs BMP, GRP-LIF vs BMP
36:4	16:0/20:4	18:2/18:2		740.5	
38:2	18:0/20:2	16:0/22:2		772.6	
38:3	18:1/20:2	18:0/20:3		770.6	
38:4	18:0/20:4	18:2/20:2		768.6	
38:5	18:1/20:4	16:0/22:5		766.5	
38:6	18:2/20:4	16:1/22:5		764.5	GRP vs BMP, GRP-LIF vs BMP
40:4	18:0/22:4	20:2/20:2		796.6	GRP-LIF vs BMP
40:5	18:0/22:5	18:1/22:4	20:1/20:4	794.6	
40:6	18:1/22:5	18:2/22:4	18:0/22:6	792.6	
40:7	18:2/22:5	20:3/20:4	18:1/22:6	790.5	
PE alkenyl-acyl species (PEp)	*Ether/acyl*			*m/z (-)*	
34:1	16:0p/18:1	18:1p/16:0		700.5	
34:2	16:0p/18:2	18:1p/16:1		698.5	
36:0	18:0/18:0			730.6	
36:1	18:0p/18:1	18:1p/18:0		728.6	
36:2	18:1p/18:1	16:0p/20:2	18:0p/18:2	726.5	
36:3	16:0p/20:3	18:1p/18:2		724.5	GRP vs BMP, LIF vs BMP, GRP-LIF vs BMP
36:4	16:0p/20:4			722.5	GRP-LIF vs BMP
38:1	18:0p/20:1			756.6	
38:2	18:0p/20:2	16:0p/22:2		754.6	
38:3	18:0p/20:3	18:1p/20:2		752.6	
38:4	18:0p/20:4	18:1p/20:3		750.5	
38:5	18:1p/20:4	16:0p/22:5		748.5	
38:6	18:1p/20:5	16:0p/22:6		746.5	
40:2	18:0p/22:2			782.6	
40:3	18:1p/22:2			780.6	
40:4	18:0p/22:4			778.6	
40:5	18:1p/22:4	18:0p/22:5		776.6	
40:6	18:1p/22:5	18:0p/22:6		774.5	

Statistical significance was determined using one-way ANOVA followed by Tukey's post hoc multiple comparison test or comparing combined groups of GRPs and LIF-stimulated A2B5+/GFAP+ with BMP-induced A2B5−/GFAP+ astrocytes by unpaired two-tailed Student's *t* test. Data are from 3 independent experiments. sn-1 Ether linkage of plasmalogen (alkenyl chain) is indicated with the letter p (e.g. 18:1p/16:0)

Discussion

We found that the lipid profiles of GRPs were altered upon astrocytic lineage differentiation induced by LIF or BMP. This work is also the first report showing that LIF-stimulated A2B5+/GFAP+ cells have a lipid composition more similar to GRPs than to BMP-induced A2B5−/GFAP+ astrocytes (Figs. 2c, 3e, 4d). The PC content was significantly reduced from GRP-LIF to BMP-induced A2B5−/GFAP+ astrocytes and SM and other simple SLs analyzed increased their proportions in parallel. Also ether PLs were elevated upon induced astrocytic lineage differentiation.

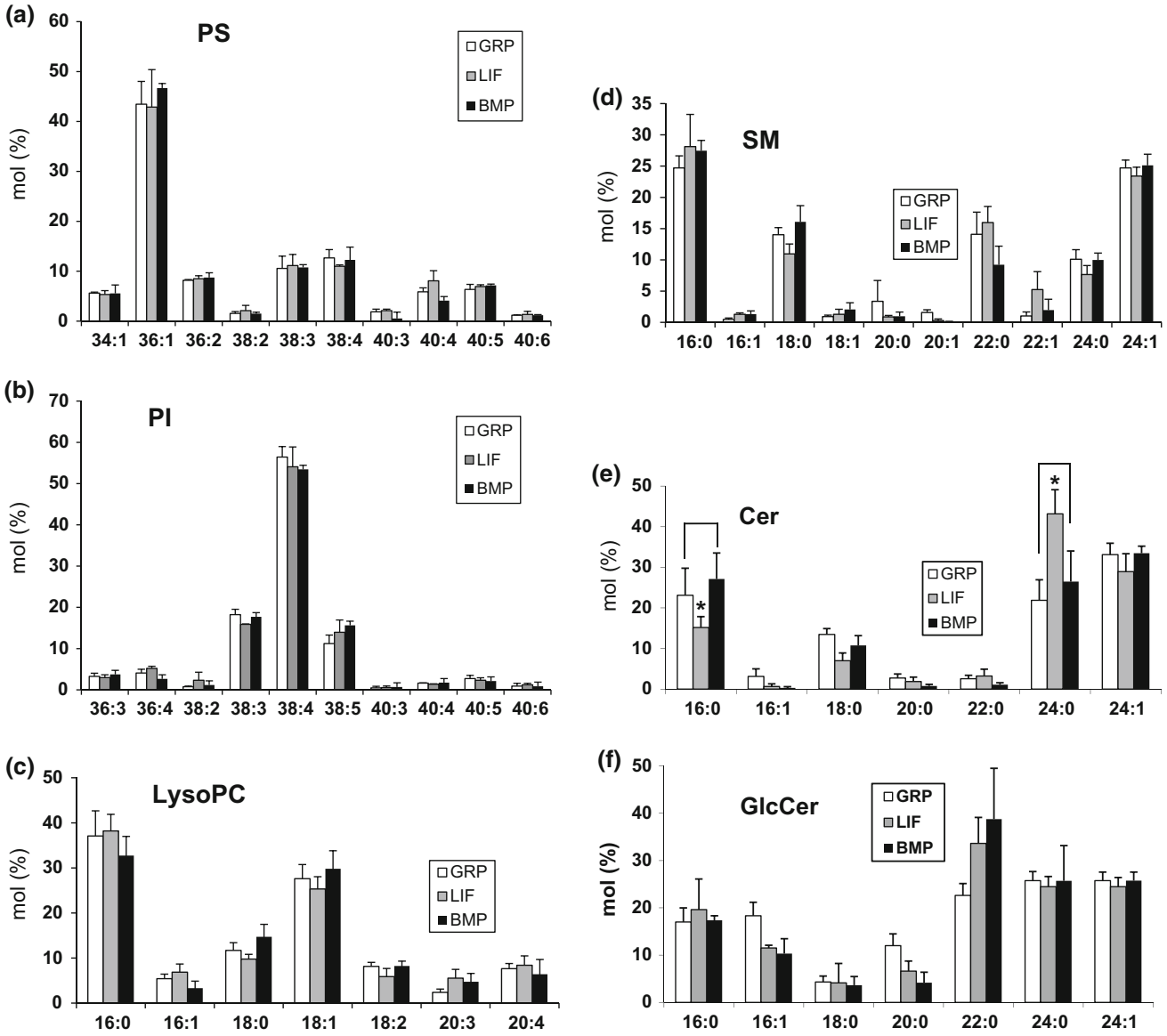

Fig. 5 Percental abundances of principal PS (**a**), PI (**b**), LysoPC (**c**), SM (**d**), Cer (**e**) or GlcCer (**f**) species in GRP, LIF-stimulated A2B5+/GFAP+ cells, and BMP-induced A2B5-/GFAP+ astrocytes. Three individual experiments were performed. Statistically significant (*t* test, $P < 0.05$) difference was marked with *asterisk*, and the comparison groups were indicated by *horizontal line*

Previously rat cerebellar granule cells were reported to have plasma membrane microdomains enriched with SLs [60]. PEp have been found to be abundant in lipid rafts [61]. Thus, the increase of SLs and PEp could indicate enhanced formation of lipid rafts in BMP-induced A2B5−/GFAP+ astrocytes.

The BMP-induced A2B5−/GFAP+ astrocytes contained elevated proportions of 20:4-containing PLs such as the 36:4 and 38:4 (16:0/20:4 and 18:0/20:4) species of PC, PCa and PEp. These PL species are the major sources of 20:4n-6 released by the action of different phospholipases A2. In cells LysoPC is the common first acceptor of 20:4n-6, which may then be converted from PC to lyso-alkenyl-PE by transacylation. The PC and PEp next release a 20:4n-6 FA upon phospholipase A2 mediated hydrolysis, thus providing a precursor for the synthesis of signaling eicosanoids, such as PGE2 [62, 63]. Apparently, the capacity of such signaling pathway is enhanced during the differentiation process. 20:4n-6 has been reported to promote neuronal differentiation and astrocytic differentiation of neural stem cells [64]. Recently, 20:4n-6-containing PC and PE were also identified as markers of the loss of stemness characteristics (e.g., capacity for immunosuppression) in human bone-marrow derived mesenchymal stem cells [53].

Ceramide synthase 2 (CERS2) has been reported to specifically produce ceramide with very long FA residues

Table 3 Principal phosphatidylserine (PS) and phosphatidylinositol (PI) molecular species

Molecular species	Identified acyl chain			*m/z* (−)
PS diacyl species	*Acyl/acyl*			
34:1	16:0/18:1			760.5
36:1	18:0/18:1			788.5
36:2	18:1/18:1			786.5
38:2	18:0/20:2			814.6
38:3	18:1/20:2			812.5
38:4	18:0/20:4	18:2/20:2		810.5
40:3	18:1/22:2	20:1/20:2		840.6
40:4	18:0/22:4	20:2/20:2		838.6
40:5	18:0/22:5	18:1/22:4	20:1/20:4	836.5
40:6	18:1/22:5	18:2/22:4	18:0/22:6	834.5
PI diacyl species				
36:3	18:1/18:2	16:0/20:3		859.5
36:4	16:0/20:4	18:2/18:2		857.5
38:2	18:0/20:2	16:0/22:2		889.6
38:3	18:1/20:2	18:0/20:3		887.6
38:4	18:0/20:4	18:2/20:2		885.6
38:5	18:1/20:4	16:0/22:5		883.5
40:3	20:1/20:3			915.6
40:4	18:0/22:4	20:2/20:2		913.6
40:5	18:0/22:5	18:1/22:4	20:1/20:4	911.6
40:6	18:1/22:5	18:2/22:4	18:0/22:6	909.6

Statistical significance was determined using one-way ANOVA followed by Tukey's post hoc multiple comparison test or comparing combined group of GRPs and LIF-stimulated A2B5+/GFAP+ with BMP-induced A2B5−/GFAP+ astrocytes by unpaired two-tailed Student's *t* test. Data are from 3 independent experiments. No statistical significance was detected in these classes

(C22–C24) [65]. Ceramides appear to be essential for neuronal development and 24:0 and 24:1 ceramides and more complex SLs produced thereof are especially important for the synthesis of myelin by oligodendrocytes [21]. LIF and CNTF promote generation, survival, and maturation of oligodendrocytes [66, 67], whereas BMP suppresses oligodendrocyte differentiation [68, 69]. In line with this, CERS2 deficient mice have defective myelin sheaths due to the reduced levels of ceramides with a long FA residue [70]. In the current study, Cer 24:0 was elevated in LIF-stimulated progenitor cells (Fig. 5e). The increase level of ceramides with very long fatty acyl moiety suggests that LIF-stimulated progenitor cells are likely to have the potential to differentiate into oligodendrocytes that are responsible for the production of CNS myelin.

BMP or LIF signaling can promote differentiation into GFAP immunoreactive cells [20, 71, 72]. GRPs and both BMP and CNTF-induced GRP differentiated cells have been transplanted into a variety of animal models [34–45]. It has been reported that these transplanted GRPs and cell derivatives of them could promote robust axonal regeneration and functional recovery. Bonaguidi et al. [31] reported that LIF and BMP signaling induce differentiation of neural stem cells into different types of GFAP+ cells. BMP-induced A2B5−/GFAP+ astrocytes have strong GFAP expression, stellate morphology and can exit the cell cycle. On the other hand, LIF-stimulated A2B5+/GFAP+ cells have a lesser GFAP immunoreactivity, do not possess stellate morphology, and do not exit the cell cycle. LIF-stimulated A2B5+/GFAP+ cells express Lewis-X carbohydrate antigenic epitope, Sox 1 and vimentin, and are capable of neurosphere formation and neuronal generation. In contrast, BMP-induced A2B5−/GFAP+ astrocytes lack these phenotypes of LIF-stimulated A2B5+/GFAP+ cells [31]. Our present data, together with those from other investigators, suggest that LIF-stimulated A2B5+/GFAP+ cells are more similar in lipid profiles as well as in cellular characteristics to stem/progenitor cells than mature astrocytes.

Two types of GFAP immunoreactive astrocytes have been described in CNS [7]. Type 1 astrocytes have been identified as GFAP+/A2B5− whereas type 2 astrocytes are GFAP+/A2B5+. GRPs can generate both types of

Table 4 Principal molecular species of lysophosphatidylcholine (LysoPC), sphingomyelin (SM), ceramide (Cer) and glucosylceramide (GlcCer)

Molecular species		*m/z* (+)
LysoPC species		
16:0		496.3
16:1		494.3
18:0		524.4
18:1		522.4
18:2		520.3
20:3		546.4
20:4		544.3
Molecular species		*m/z* (+)
Base/acyl		
Cer species		
18:1/16:0	16:1/18:0	538.5
18:1/16:1		536.5
18:1/18:0		566.6
18:1/20:0		594.6
18:1/22:0	20:1/18:0	622.6
18:1/24:0	20:1/22:0	650.6
18:1/24:1	20:1/22:1	648.6
SM species		
18:1/16:0	16:1/18:0	703.6
18:1/16:1		701.6
18:1/18:0		731.6
18:1/18:1	18:2/18:0	729.6
18:1/20:0		759.6
18:1/20:1		757.6
18:1/22:0	20:1/18:0	787.7
18:1/22:1		785.7
18:1/24:0	20:1/22:0	815.7
18:1/24:1	20:1/22:1	813.7
GlcCer species		
18:1/16:0	16:1/18:0	700.6
18:1/16:1		698.6
18:1/18:0		728.6
18:1/20:0		756.6
18:1/22:0	20:1/18:0	784.7
18:1/24:0	20:1/22:0	812.7

Statistical significance was determined using one-way ANOVA followed by Tukey's post hoc multiple comparison test or comparing combined group of GRPs and LIF-stimulated A2B5+/GFAP+ with BMP-induced A2B5−/GFAP+ astrocytes by unpaired two-tailed Student's *t* test. Data from 3 independent experiments. No significant differences were detected in these classes

astrocytes. In the present study, BMP-induced A2B5−/GFAP+ astrocytes are considered as type 1 astrocytes and the LIF-stimulated A2B5+/GFAP+ cells are referred to as

Table 5 Molar proportions (%) of the most abundant lipid acyl (detected as fatty acid methyl esters) and alkenyl (detected as dimethyl acetal, DMA) residues

Acyl	GRP	LIF	BMP
SUM SFA	35.6	34.7	37.2
14:0	1.3	1.0	0.8
15:0	0.3	0.3	0.3
16:0	20.5	21.2	21.6
17:0	3.1	2.6	3.7
18:0	9.4	8.6	9.1
19:0	0.1	0.1	0.1
20:0	0.2	0.2	0.2
22:0	0.2	0.3	0.3
24:0	0.5	0.5	1.2
SUM MUFA	30.5	24.7	24.1
SUM 16:1	3.2	2.8	2.3
16:1n-9	1.4	1.1	1.0
16:1n-7	1.8	1.8	1.3
17:1n-8	0.1	0.2	0.2
SUM 18:1	24.3	18.8	18.0
18:1n-9	17.9	13.0	12.2
18:1n-7	6.1	5.5	5.5
18:1n-5	0.3	0.3	0.2
19:1n-10	0.5	0.4	0.6
SUM 20:1	1.3	1.2	1.4
20:1n-11	0.2	0.6	0.6
20:1n-9	0.7	0.4	0.6
20:1n-7	0.4	0.2	0.2
SUM 22:1	0.2	0.2	0.4
22:1n-11	0.1	0.1	0.2
22:1n-9	0.1	0.1	0.2
24:1n-9	0.9	1.0	1.3
SUM PUFA	28.0	33.4	31.2
18:2n-6	5.1	6.7	4.7
SUM 20:2	6.3	5.2	4.6
20:2n-9	4.9	3.6	3.1
20:2n-6	1.5	1.6	1.5
SUM 20:3	1.9	1.6	1.4
20:3n-9	0.8	0.7	0.5
20:3n-6	1.1	0.9	0.9
SUM 20:4	8.3	10.7	13.7
20:4n-6	6.8	7.4	10.1
20:4n-3	1.5	3.4	3.6
20:5n-3	0.7	0.7	0.4
22:2	1.3	2.4	0.2
22:3	0.5	0.6	1.9
22:4n-6	1.5	1.7	1.1
SUM 22:5	2.4	3.7	3.1
22:5n-6	0.9	2.2	1.0
22:5n-3	1.4	1.6	2.1
22:6n-3	0.6	0.6	0.6

Table 5 continued

Acyl	GRP	LIF	BMP
SUM n-6	15.4	18.4	17.8
SUM n-3	4.1	5.8	6.5
n-3/n-6 PUFA	0.3	0.3	0.4
Alkenyl	GRP	LIF	BMP
SUM DMA	6.6	7.5	8.6
16:0 DMA	2.4	2.7	3.4
18:0 DMA	1.4	1.4	1.7
18:1 DMA	2.8	3.4	3.6

SFA Saturated fatty acids, *MUFA* monounsaturated fatty acids, *PUFA* polyunsaturated fatty acids, *DMA* dimethylacetal, derivative of alkenyl chain. The values represent average of two independent experiments (n = 2)

type 2 astrocytes. A subpopulation of type 2 astrocytes has been reported to be multipotent, and these cells share common properties as neural stem cells [73]. The present study establishes the lipidomic profiles characteristic of two different GFAP+ cells derived from GRPs of rat spinal cord and it also shows that LIF-stimulated A2B5+/GFAP+ cells have the lipid composition more similar to GRP than BMP-induced A2B5−/GFAP+ astrocytes. The different contents of specific SLs and ether or diacyl PL species containing 20:4n-6 likely indicate a functional correlation between the lipidomes and cellular functions. However, additional studies are required to establish such correlations, the underlying mechanisms and their relevance in vivo. A tempting view is that different progenitor cells share certain common lipidomic characteristics. For this reason, we predict that the lipid profiles could be used to study the spatial distributions and functions of different astrocyte and progenitor populations in different parts of CNS at different developmental stages and/or in pathogenic mechanism of CNS diseases, e.g., by monitoring these lipids in cryosections of nervous tissue using time-of-flight secondary ion mass spectrometry (TOF–SIMS) [74]. Further systematic studies focusing on the functional roles of the lipid composition and specific lipids in progenitor cells and in differentiated cells are needed to advance our knowledge of stem cell biology.

Acknowledgments We thank Agnès Viherä, Lea Armassalo, Tarja Grundström, Eliisa Kekäläinen, Aaro Miettinen, and Johanna Mäkelä for excellent technical assistance, the Molecular Imaging Unit of Biomedicum Helsinki for the use of their instrument and for assistance, and Dr. Masaaki Kitada for helpful comments on this research. This work was supported in part by a fellowship funding from Academy of Finland (No. 111261 to RK), grants from Japan Brain Foundation (YI), the Nakayama Foundation of Human Science (YI), and the Mizutani Foundation for Glycoscieince (150026 to YI).

References

1. Jayakumar AR, Tong XY, Curtis KM, Ruiz-Cordero R, Shamaladevi N, Abuzamel M, Johnstone J, Gaidosh G, Rama Rao KV, Norenberg MD (2014) Decreased astrocytic thrombospondin-1 secretion after chronic ammonia treatment reduces the level of synaptic proteins: in vitro and in vivo studies. J Neurochem 131:333–347
2. Rodnight RB, Gottfried C (2013) Morphological plasticity of rodent astroglia. J Neurochem 124:263–275
3. Sofroniew MV, Vinters HV (2010) Astrocytes: biology and pathology. Acta Neuropathol 119:7–35
4. Tsai HH, Li H, Fuentealba LC, Molofsky AV, Taveira-Marques R, Zhuang H, Tenney A, Murnen AT, Fancy SP, Merkle F, Kessaris N, Alvarez-Buylla A, Richardson WD, Rowitch DH (2012) Regional astrocyte allocation regulates CNS synaptogenesis and repair. Science 337:358–362
5. Eisenbarth GS, Walsh FS, Nirenberg M (1979) Monoclonal antibody to a plasma membrane antigen of neurons. Proc Natl Acad Sci USA 76:4913–4917
6. Kasai N, Yu RK (1983) The monoclonal antibody A2B5 is specific to ganglioside GQ1c. Brain Res 277:155–158
7. Raff MC, Abney ER, Cohen J, Lindsay R, Noble M (1983) Two types of astrocytes in cultures of developing rat white matter: differences in morphology, surface gangliosides, and growth characteristics. J Neurosci 3:1289–1300
8. Saito M, Kitamura H, Sugiyama K (2001) The specificity of monoclonal antibody A2B5 to c-series gangliosides. J Neurochem 78:64–74
9. Viljetic B, Labak I, Majic S, Stambuk A, Heffer M (2012) Distribution of mono-, di- and trisialo gangliosides in the brain of Actinopterygian fishes. Biochim Biophys Acta 1820:1437–1443
10. Kishimoto N, Shimizu K, Sawamoto K (2012) Neuronal regeneration in a zebrafish model of adult brain injury. Dis Model Mech 5:200–209
11. Itokazu Y, Yu RK (2014) Amyloid beta-peptide 1-42 modulates the proliferation of mouse neural stem cells: upregulation of fucosyltransferase IX and Notch signaling. Mol Neurobiol 50:186–196
12. Ando S, Yu RK (1979) Isolation and characterization of two isomers of brain tetrasialogangliosides. J Biol Chem 254:12224–12229
13. Freischutz B, Saito M, Rahmann H, Yu RK (1994) Activities of five different sialyltransferases in fish and rat brains. J Neurochem 62:1965–1973
14. Freischutz B, Saito M, Rahmann H, Yu RK (1995) Characterization of sialyltransferase-IV activity and its involvement in the c-pathway of brain ganglioside metabolism. J Neurochem 64:385–393
15. Yu RK, Itokazu Y (2014) Glycolipid and glycoprotein expression during neural development. Adv Neurobiol 9:185–222
16. Ngamukote S, Yanagisawa M, Ariga T, Ando S, Yu RK (2007) Developmental changes of glycosphingolipids and expression of glycogenes in mouse brains. J Neurochem 103:2327–2341
17. Yu RK, Nakatani Y, Yanagisawa M (2009) The role of glycosphingolipid metabolism in the developing brain. J Lipid Res 50(Suppl):S440–S445
18. Rao MS, Mayer-Proschel M (1997) Glial-restricted precursors are derived from multipotent neuroepithelial stem cells. Dev Biol 188:48–63
19. Bieberich E (2012) It's a lipid's world: bioactive lipid metabolism and signaling in neural stem cell differentiation. Neurochem Res 37:1208–1229
20. ten Grotenhuis E, Demel RA, Ponec M, Boer DR, van Miltenburg JC, Bouwstra JA (1996) Phase behavior of stratum corneum

lipids in mixed Langmuir-Blodgett monolayers. Biophys J 71:1389–1399
21. Grosch S, Schiffmann S, Geisslinger G (2012) Chain length-specific properties of ceramides. Prog Lipid Res 51:50–62
22. Gross RE, Mehler MF, Mabie PC, Zang Z, Santschi L, Kessler JA (1996) Bone morphogenetic proteins promote astroglial lineage commitment by mammalian subventricular zone progenitor cells. Neuron 17:595–606
23. Rajan P, McKay RD (1998) Multiple routes to astrocytic differentiation in the CNS. J Neurosci 18:3620–3629
24. Marks DL, Bittman R, Pagano RE (2008) Use of Bodipy-labeled sphingolipid and cholesterol analogs to examine membrane microdomains in cells. Histochem Cell Biol 130:819–832
25. Simons K, Ikonen E (1997) Functional rafts in cell membranes. Nature 387:569–572
26. Tajima N, Itokazu Y, Korpi ER, Somerharju P, Käkelä R (2011) Activity of BK(Ca) channel is modulated by membrane cholesterol content and association with Na+/K+-ATPase in human melanoma IGR39 cells. J Biol Chem 286:5624–5638
27. Lee MY, Ryu JM, Lee SH, Park JH, Han HJ (2010) Lipid rafts play an important role for maintenance of embryonic stem cell self-renewal. J Lipid Res 51:2082–2089
28. Yanagisawa M, Nakamura K, Taga T (2004) Roles of lipid rafts in integrin-dependent adhesion and gp130 signalling pathway in mouse embryonic neural precursor cells. Genes Cells 9:801–809
29. Yang C, Ji L, Yue W, Wang RY, Li YH, Xi JF, Xie XY, He LJ, Nan X, Pei XT (2010) Erythropoietin gene-modified conditioned medium of human mesenchymal cells promotes hematopoietic development from human embryonic stem cells. J Exp Hematol/Chin Assoc Pathophysiol 18:976–980
30. Bouffi C, Bony C, Courties G, Jorgensen C, Noel D (2010) IL-6-dependent PGE2 secretion by mesenchymal stem cells inhibits local inflammation in experimental arthritis. PLoS ONE 5:e14247
31. Bonaguidi MA, McGuire T, Hu M, Kan L, Samanta J, Kessler JA (2005) LIF and BMP signaling generate separate and discrete types of GFAP-expressing cells. Development 132:5503–5514
32. Kang JX, Wan JB, He C (2013) Regulation of stem cell proliferation and differentiation by essential fatty acids and their metabolites. Stem Cells 32:1092–1098
33. Doria ML, Cotrim Z, Macedo B, Simoes C, Domingues P, Helguero L, Domingues MR (2012) Lipidomic approach to identify patterns in phospholipid profiles and define class differences in mammary epithelial and breast cancer cells. Breast Cancer Res Treat 133:635–648
34. Alexanian AR, Svendsen CN, Crowe MJ, Kurpad SN (2011) Transplantation of human glial-restricted neural precursors into injured spinal cord promotes functional and sensory recovery without causing allodynia. Cytotherapy 13:61–68
35. Davies JE, Huang C, Proschel C, Noble M, Mayer-Proschel M, Davies SJ (2006) Astrocytes derived from glial-restricted precursors promote spinal cord repair. J Biol 5:7
36. Davies JE, Proschel C, Zhang N, Noble M, Mayer-Proschel M, Davies SJ (2008) Transplanted astrocytes derived from BMP- or CNTF-treated glial-restricted precursors have opposite effects on recovery and allodynia after spinal cord injury. J Biol 7:24
37. Davies SJ, Shih CH, Noble M, Mayer-Proschel M, Davies JE, Proschel C (2011) Transplantation of specific human astrocytes promotes functional recovery after spinal cord injury. PLoS ONE 6:e17328
38. Haas C, Fischer I (2013) Human astrocytes derived from glial restricted progenitors support regeneration of the injured spinal cord. J Neurotrauma 30:1035–1052
39. Haas C, Neuhuber B, Yamagami T, Rao M, Fischer I (2012) Phenotypic analysis of astrocytes derived from glial restricted precursors and their impact on axon regeneration. Exp Neurol 233:717–732
40. Han SS, Liu Y, Tyler-Polsz C, Rao MS, Fischer I (2004) Transplantation of glial-restricted precursor cells into the adult spinal cord: survival, glial-specific differentiation, and preferential migration in white matter. Glia 45:1–16
41. Hill CE, Proschel C, Noble M, Mayer-Proschel M, Gensel JC, Beattie MS, Bresnahan JC (2004) Acute transplantation of glial-restricted precursor cells into spinal cord contusion injuries: survival, differentiation, and effects on lesion environment and axonal regeneration. Exp Neurol 190:289–310
42. Jin Y, Neuhuber B, Singh A, Bouyer J, Lepore A, Bonner J, Himes T, Campanelli JT, Fischer I (2011) Transplantation of human glial restricted progenitors and derived astrocytes into a contusion model of spinal cord injury. J Neurotrauma 28:579–594
43. Lepore AC, Neuhuber B, Connors TM, Han SS, Liu Y, Daniels MP, Rao MS, Fischer I (2006) Long-term fate of neural precursor cells following transplantation into developing and adult CNS. Neuroscience 139:513–530
44. Porambo M, Phillips AW, Marx J, Ternes K, Arauz E, Pletnikov M, Wilson MA, Rothstein JD, Johnston MV, Fatemi A (2015) Transplanted glial restricted precursor cells improve neurobehavioral and neuropathological outcomes in a mouse model of neonatal white matter injury despite limited cell survival. Glia 63:452–465
45. Walczak P, All AH, Rumpal N, Gorelik M, Kim H, Maybhate A, Agrawal G, Campanelli JT, Gilad AA, Kerr DA, Bulte JW (2011) Human glial-restricted progenitors survive, proliferate, and preserve electrophysiological function in rats with focal inflammatory spinal cord demyelination. Glia 59:499–510
46. Rao MS, Noble M, Mayer-Proschel M (1998) A tripotential glial precursor cell is present in the developing spinal cord. Proc Natl Acad Sci USA 95:3996–4001
47. Li H, Grumet M (2007) BMP and LIF signaling coordinately regulate lineage restriction of radial glia in the developing forebrain. Glia 55:24–35
48. Noble M, Davies JE, Mayer-Proschel M, Proschel C, Davies SJ (2011) Precursor cell biology and the development of astrocyte transplantation therapies: lessons from spinal cord injury. Neurotherapeutics 8:677–693
49. Folch J, Lees M, Sloane Stanley GH (1957) A simple method for the isolation and purification of total lipides from animal tissues. J Biol Chem 226:497–509
50. Hermansson M, Käkelä R, Berghäll M, Lehesjoki AE, Somerharju P, Lahtinen U (2005) Mass spectrometric analysis reveals changes in phospholipid, neutral sphingolipid and sulfatide molecular species in progressive epilepsy with mental retardation, EPMR, brain: a case study. J Neurochem 95:609–617
51. Hermansson M, Uphoff A, Käkelä R, Somerharju P (2005) Automated quantitative analysis of complex lipidomes by liquid chromatography/mass spectrometry. Anal Chem 77:2166–2175
52. Käkelä R, Somerharju P, Tyynelä J (2003) Analysis of phospholipid molecular species in brains from patients with infantile and juvenile neuronal-ceroid lipofuscinosis using liquid chromatography-electrospray ionization mass spectrometry. J Neurochem 84:1051–1065
53. Kilpinen L, Tigistu-Sahle F, Oja S, Greco D, Parmar A, Saavalainen P, Nikkila J, Korhonen M, Lehenkari P, Käkelä R, Laitinen S (2013) Aging bone marrow mesenchymal stromal cells have altered membrane glycerophospholipid composition and functionality. J Lipid Res 54:622–635
54. Koivusalo M, Haimi P, Heikinheimo L, Kostiainen R, Somerharju P (2001) Quantitative determination of phospholipid compositions by ESI-MS: effects of acyl chain length, unsaturation, and lipid concentration on instrument response. J Lipid Res 42:663–672
55. Brügger B, Erben G, Sandhoff R, Wieland FT, Lehmann WD (1997) Quantitative analysis of biological membrane lipids at the

low picomole level by nano-electrospray ionization tandem mass spectrometry. Proc Natl Acad Sci USA 94:2339–2344
56. Sullards MC, Merrill AH Jr (2001) Analysis of sphingosine 1-phosphate, ceramides, and other bioactive sphingolipids by high-performance liquid chromatography-tandem mass spectrometry. Sci STKE 67:l1
57. Haimi P, Uphoff A, Hermansson M, Somerharju P (2006) Software tools for analysis of mass spectrometric lipidome data. Anal Chem 78:8324–8331
58. Käkelä R, Käkelä A, Kahle S, Becker PH, Kelly A, Furness RW (2005) Fatty acid signatures in plasma of captive herring gulls as indicators of demersal or pelagic fish diet. Mar Ecol Prog Ser 293:191–200
59. Kvalheim OM, Karstang TV (1987) A General-purpose program for multivariate data-analysis. Chemometr Intell Lab 2:235–237
60. Prinetti A, Chigorno V, Tettamanti G, Sonnino S (2000) Sphingolipid-enriched membrane domains from rat cerebellar granule cells differentiated in culture. A compositional study. J Biol Chem 275:11658–11665
61. Pike LJ, Han X, Chung KN, Gross RW (2002) Lipid rafts are enriched in arachidonic acid and plasmenylethanolamine and their composition is independent of caveolin-1 expression: a quantitative electrospray ionization/mass spectrometric analysis. Biochemistry 41:2075–2088
62. Chilton FH, Fonteh AN, Surette ME, Triggiani M, Winkler JD (1996) Control of arachidonate levels within inflammatory cells. Biochim Biophys Acta 1299:1–15
63. Diez E, Chilton FH, Stroup G, Mayer RJ, Winkler JD, Fonteh AN (1994) Fatty acid and phospholipid selectivity of different phospholipase A2 enzymes studied by using a mammalian membrane as substrate. Biochem J 301(Pt 3):721–726
64. Sakayori N, Maekawa M, Numayama-Tsuruta K, Katura T, Moriya T, Osumi N (2011) Distinctive effects of arachidonic acid and docosahexaenoic acid on neural stem/progenitor cells. Genes Cells 16:778–790
65. Mizutani Y, Kihara A, Igarashi Y (2005) Mammalian Lass6 and its related family members regulate synthesis of specific ceramides. Biochem J 390:263–271
66. Adachi T, Takanaga H, Kunimoto M, Asou H (2005) Influence of LIF and BMP-2 on differentiation and development of glial cells in primary cultures of embryonic rat cerebral hemisphere. J Neurosci Res 79:608–615
67. Mayer M, Bhakoo K, Noble M (1994) Ciliary neurotrophic factor and leukemia inhibitory factor promote the generation, maturation and survival of oligodendrocytes in vitro. Development 120:143–153
68. Mabie PC, Mehler MF, Kessler JA (1999) Multiple roles of bone morphogenetic protein signaling in the regulation of cortical cell number and phenotype. J Neurosci 19:7077–7088
69. Yung SY, Gokhan S, Jurcsak J, Molero AE, Abrajano JJ, Mehler MF (2002) Differential modulation of BMP signaling promotes the elaboration of cerebral cortical GABAergic neurons or oligodendrocytes from a common sonic hedgehog-responsive ventral forebrain progenitor species. Proc Natl Acad Sci USA 99:16273–16278
70. Imgrund S, Hartmann D, Farwanah H, Eckhardt M, Sandhoff R, Degen J, Gieselmann V, Sandhoff K, Willecke K (2009) Adult ceramide synthase 2 (CERS2)-deficient mice exhibit myelin sheath defects, cerebellar degeneration, and hepatocarcinomas. J Biol Chem 284:33549–33560
71. Fukuda S, Taga T (2005) Cell fate determination regulated by a transcriptional signal network in the developing mouse brain. Anat Sci Int 80:12–18
72. Nakashima K, Yanagisawa M, Arakawa H, Kimura N, Hisatsune T, Kawabata M, Miyazono K, Taga T (1999) Synergistic signaling in fetal brain by STAT3-Smad1 complex bridged by p300. Science 284:479–482
73. Kondo T, Raff M (2000) Oligodendrocyte precursor cells reprogrammed to become multipotential CNS stem cells. Science 289:1754–1757
74. Sjövall P, Lausmaa J, Johansson B (2004) Mass spectrometric imaging of lipids in brain tissue. Anal Chem 76:4271–4278